batteries

MDPI

Article

Perfluorosulfonic Acid Membrane for Lithium–Sulfur Batteries with S/C Cathodes †

Andrey B. Yaroslavtsev [1,*], Svetlana A. Novikova [1], Daria Yu. Voropaeva [1], Sergey A. Li [2,3] and Tatiana L. Kulova [2]

[1] Kurnakov Institute of General and Inorganic Chemistry, Russian Academy of Sciences, 31 Leninskii pr., 119991 Moscow, Russia
[2] Frumkin Institute of Physical Chemistry and Electrochemistry, Russian Academy of Sciences, 31-4 Leninskii pr., 119071 Moscow, Russia
[3] Moscow Power Engineering Institute, National Research University, Krasnokazarmennaya Str. 14, 111250 Moscow, Russia
* Correspondence: yaroslav@igic.ras.ru
† This paper is an extended version of our paper published in the 1st International Electronic Conference on Processes: Processes System Innovation, 17–31 May 2022.

Abstract: Polymer electrolyte based on Nafion-117 membranes in the Li^+ form with intercalated 1,3-dioxolane-dimethoxyethane solvent mixtures (DOL-DME) has been obtained. The obtained electrolyte Nafion-Li^+-DOL-DME has been characterized by DSC analysis, IR- and impedance spectroscopy. The solvent uptake of membrane in the DOL-DME mixture amounts to 1.9. Nafion-Li^+-DOL-DME is characterized by an ionic conductivity ~10^{-7} S cm^{-1} at room temperature. The comparative study of the electrochemical properties of Li–S batteries with liquid electrolyte (1M $Li(CF_3SO_2)_2N$ in DOL-DME) with polypropylene film (PP) or Nafion-Li^+-DOL-DME and S/C composites with mesoporous carbon as cathode materials has shown that the use of membrane can improve cyclability of the cell. The first-cycle discharge capacities of S/C electrodes in the Li–S battery cells with PP and Nafion-Li^+-DOL-DME were 730 and 450 mAh g^{-1}, respectively (0.1 mV s^{-1}). However, the discharge capacity of S/C in the cell with PP reduced significantly after 10 cycles. The Li–S battery with the use of membrane exhibits significantly enhanced cyclability. The discharge capacity of S/C in the cell with Nafion-Li^+-DOL-DME amounts to 365 mAh g^{-1} after 10 cycles and to up to 290 mAh g^{-1} after 40 cycles.

Keywords: Li–S battery; ion exchange membrane; solvent uptake; conductivity; selectivity

Citation: Yaroslavtsev, A.B.; Novikova, S.A.; Voropaeva, D.Y.; Li, S.A.; Kulova, T.L. Perfluorosulfonic Acid Membrane for Lithium–Sulfur Batteries with S/C Cathodes. *Batteries* **2022**, *8*, 162. https://doi.org/10.3390/batteries8100162

Academic Editor: Claudio Gerbaldi

Received: 31 August 2022
Accepted: 3 October 2022
Published: 6 October 2022

1. Introduction

Lithium–sulfur (Li–S) batteries promise a much higher capacity compared to common Li-ion batteries (theoretical capacity of Li and S amount to 3860 and 1672 mAh g^{-1}) [1]. Sulfur undergoes a conversion reaction with the formation of lithium polysulfides [2], allowing for the possible introduction of two lithium cations and electrons per sulfur atom [3]. At the same time, sulfur is an abundant, low-cost, and non-toxic element. This explains the interest in Li–S batteries. Unfortunately, a few issues are still hindering their wide commercial application. Among them, the low electrical conductivity of sulfur, significant change in the volume of the cathode during the discharge/charge process, and the migration of soluble lithium polysulfides between electrodes should be mentioned [4,5]. Much attention has been paid to the development of materials for lithium–sulfur batteries. The shuttle effect reduction is the most important among the above-mentioned problems. Approaches such as composite cathode formation with carbon materials, covalent bonding of sulfur, the use of cathodes with addition of electrocatalyst, inserting a selective separators or supplementary interlayer are used to overcome this problem [4,5].

Due to the system of pore and channels with the size of several nanometers containing functional groups that determine the transport properties of the membranes [6],

ion-exchange membranes are considered to be promising materials for various applications. The main fields of their use include electrodialysis, desalination and the concentration of electrolyte solutions [7], for example for the recovery of monovalent cations [8,9] as well as application in alternative renewable energy sources such as fuel cells [10], reverse electrodialysis [11] and vanadium redox flow batteries [12]. Nafion represents a copolymer of perfluoro-vinyl-ether and tetrafluoroethylene. Nafion is widely used in its hydrated state in proton exchange membrane fuel cells due to its high proton conductivity and excellent stability. Cheaper cation-exchange materials are being intensively developed, for example, based on functionalized or sulfonated polystyrene [13]. When converted to lithium form, the membrane becomes a Li^+ conductor. Solvation with aprotic organic solvents makes it possible to use the cation-exchange membranes in metal-ion batteries as an electrolyte [14,15], a conductive binder [15,16] or for anode protection in batteries with lithium anode [17]. There are several studies demonstrating the possibility the possibility of using cation-exchange membranes in metal-sulfur batteries for reducing the polysulfide shuttle effect. The functional SO_3^- groups allow Li^+ or Na^+ mobility but prevent transport of negative ions, such as polysulfide anions (S_n^{2-}). Cation exchange membranes are used instead of a liquid electrolyte [18], in combination with liquid electrolytes instead of porous separator [19], for modification of separator [20–25] or for coating of positive electrode [26,27]. It is shown that the transfer of alkali metal polysulfides between the electrodes can be significantly reduced and the cycling stability of battery cell improved with the use of cation-exchange materials.

Conductivity of Nafion-type membranes depends on the degree of solvation and the nature of the sorbed organic solvent [28]. The solvent uptake, in turn, depends on the conditions of its pretreatment, the nature of the sorbed solvent, the presence and concentration of the dissolved salt in the solvent [29] and on the membrane itself. For example, the conductivity values of Nafion-112-Li^+ intercalated by EC-PC mixture is 8×10^{-5} S cm^{-1} (room temperature) [30]. Nepem membrane (analogous to Nafion, Yixing, Jiangsu, China) soaked in the same mixture EC-PC is characterized by a higher conductivity (7×10^{-4} S cm^{-1}) [31]. The incorporation of solvents such as organic carbonates [31], dimethyl sulfoxide [32], and mixtures based on organic carbonates-dimethylacetamide [33], ethylene carbonate-sulfolane [34,35] are carefully described. Varying the compositions of solvents makes it possible to obtain higher values of the solvent uptake and, accordingly, ionic conductivity. Ionic conductivity increases in the series diethyl carbonate~dimethyl carbonate (DMC)~DME~tetrahydrofurane~DOL~acetonitrile~gamma-butyrolactone < ethylene carbonate—dimethyl carbonate—diethyl carbonate < propylene carbonate < ethylene carbonate—propylene carbonate < ethylene carbonate—DME < dimethylformamide ~ dimethyl sulfoxide < ethylene carbonate—diethyl carbonate—dimethylacetamide < ethylene carbonate—propylene carbonate—dimethylacetamide—tetrahydrofuran < ethylene carbonate—propylene carbonate—dimethylacetamide [28]. This is due to the combination of such characteristics of the solvents and their mixtures as viscosity and dielectric constant. However, organic carbonate-based electrolytes react irreversibly with polysulfides [36]. The problem of compatibility between organic carbonate-based solvents and polysulfides can be minimized by using specially designed cathodes that are capable of preventing the formation of soluble polysulfides [37]. With that, ethers do not react with polysulfides, unlike organic carbonates [36,38]. DOL-DME mixture is one of the most successfully employed and most commonly used as a solvent for Li–S batteries [2].

At the same time, there is little data in the literature on the solvation and transport characteristics of the Nafion membrane intercalated by the DOL-DME mixture. This work is devoted to the study of the swelling, thermal stability, mechanical strength, conductivity and selectivity of Nafion membranes in Li^+ form intercalated by DOL-DME mixture (Nafion-Li^+-DOL-DME). Such investigation of the lithiated Nafion intercalated by the DOL-DME mixture is performed for the first time. The comparative study of the electrochemical properties of Li–S batteries with a liquid electrolyte (1M $Li(CF_3SO_2)_2N$ in DOL-DME) with a polypropylene film (PP) or Nafion-Li^+-DOL-DME and S/C composites

with mesoporous carbon as cathode materials is performed. It is shown that the use of membranes can significantly improve the cyclability of the cell.

2. Materials and Methods

Mesoporous carbon was obtained from NanoTechCenter LTD (Tambov, Russia). It was purified from remainders of the catalyst used in the synthesis according to the manufacturer's procedures: material was treated with 30% (by weight) HNO_3 in weight ratio of 1:8 for 1 h at 90 °C with constant stirring. After that, it was washed with deionized water to pH~7 and dried in air for 24 h at 90 °C.

S/C composite material was prepared by the conventional melt diffusion method. The mesoporous carbon was ground with elemental sulfur in a mass ratio of 1:1 The mixture was kept for 20 h at 155 °C in Ar atmosphere in a Teflon-lined reactor.

The Nafion-117 membranes were industrially obtained (Dupont, Wilmington, NC, USA); ion exchange capacity is 0.91 m-eq g^{-1}, and the thickness of the dry membranes is ~180 μm. Anhydrous aprotic solvents with the purity grade > 99.7% were used. The membranes were conditioned by a standard procedure [39], soaked in 0.1M lithium hydroxide solution and kept for 24 h with constant stirring with a threefold change of the solution. The membranes were washed several times with deionized water to remove OH^- ions. The membranes were then dried at 50 °C under vacuum for 12 h to remove water. The obtained dried samples were placed into a dry argon-filled box and were soaked in DOL-DME mixture (1:1 by volume) to fill the pores of the membranes with aprotic solvents. The membranes were kept in the mentioned solutions over molecular sieves (3 Å) for 1–14 days. All manipulations were performed in a glove box under argon atmosphere. Contents of O_2 and H_2O in the box were less than 1 ppm.

X-ray diffraction (XRD) analysis was carried out with the use of a Rigaku D/MAX 2200 diffractometer (CuKα, Rigaku, Tokyo, Japan). The XRD patterns were analyzed with the use of Rigaku Application Data Processing software. The percent crystallinity (X_{cr}) was investigated using Equation (1) [40]:

$$X_{\mathrm{cr}} = \frac{A_{cr}}{A_{cr} + A_{am}} \quad (1)$$

where A_c and A_{am} are the areas of crystalline and amorphous peaks, respectively. The decomposition of the peaks was performed with the use of Gauss function after subtraction of the background profile from the original X-ray profile.

Microstructure analysis of the samples was completed with the use of a scanning electron microscope (SEM) TESCAN AMBER GMH (TESCAN, Brno, Czech Republic). The specific surface area was determined by the BET method using a Sorbtometer-M analyzer (LLC Katakon, Novosibirsk, Russia). Raman spectra were collected using DXRxi Raman Imaging Microscope (Thermo Fisher Scientific, Madison, WI, USA).

The solvent uptake of the membranes (n) was calculated as a ratio of the number of the solvent molecules to the number of sulfonic groups of membrane. For this purpose, mass gain after soaking the membranes in the solvents was measured, assuming that the composition of the sorbed mixture is the same as the contacting solution. To assess the effect of solvation time on the solvent uptake and ionic conductivity of the membranes, they were kept in DOL-DME for 1, 3, 5, 7, and 14 days.

Swelling of the membranes (Δm, %) was calculated by Equation (2):

$$\Delta m = \frac{m - m_0}{m_0} \cdot 100 \quad (2)$$

where m_0 and m are the weight of the dry and solvated membranes, respectively.

Solvation degree, which is the number of solvent molecules per one functional group, was determined based on ion-exchange capacity and swelling by Equation (3)

$$n = \frac{\Delta m \cdot 10}{IEC \cdot M_{solvent}} \quad (3)$$

where Δm is the membrane' swelling (%), IEC is ion-exchange capacity (mmol g^{-1}), $M_{solvent}$ is the average molecular weight of the DOL-DME mixture (81.29 g mol^{-1}).

IR spectra of the membranes were obtained using a Nicolet iS5 FTIR (Thermo Fisher Scientific, Madison, WI, USA) with a Quest Specac diamond crystal attachment (spectral range 500–4000 cm^{-1}, 32 scans, 2 cm^{-1} resolution) in the attenuated total reflection mode.

The mechanical properties of the solvated membranes were investigated by stress–strain curves using a Tinius Olsen H5KT tensile testing machine. Measurements were performed on rectangular samples 30 mm long and 9–11 mm wide. The experiment was conducted three times for membrane sample. The average values of Young's modulus and tensile strength were determined from the three values. Before the experiment, the thickness and width of each sample were measured as 3-point averages. The calibration length of the samples was 17 mm. The strain rate was 2 mm min^{-1}. Young's modulus was calculated from the slope of the stress–strain curve in the region of reversible deformations. Measurement errors were calculated according to Student's *t*-test with a 95% confidence level.

Ionic conductivity of the obtained samples was investigated by impedance spectroscopy in the temperature range of 0 … +50 °C under an argon atmosphere. The climate chamber Binder MKF115 was used to obtain the required temperatures. Measurements were carried out using the Elins Z-1500 J alternating current bridge (Elins, Chernogolovka, Russia) in the frequency range 2 MHz—10 Hz on stainless steel/membrane/stainless steel in a CR2032 coin-type cell. Resistances were determined by an intercept with the active impedance axis in Nyquist coordinates. Linear dependence of ionic conductivity on temperature in the Arrhenius coordinates logσ—1000/T was used for the calculation of the activation energy of conductivity.

Differential scanning calorimetry (DSC) of the solvated membrane was performed on a NETZSCH STA 449F1 (NETZSCH, Selb, Germany) in aluminum crucibles in a helium atmosphere (flow rate was 20 mL min^{-1}) in the temperature range −100–+130 °C with heating rate 10 °C min^{-1}.

The Li^+ transference number was evaluated by the Bruce-Vincent method [41] in a symmetrical Li/Nafion-Li+-DOL-DME/Li coin cell using Elins P-20X8 (Elins, Russia). The cell was polarized by a direct current (ΔV = 10 mV). The current value in steady state (I_{ss}) was obtained by extrapolation to infinite time the experimentally recorded chronoamperometry curve. The interfacial resistance was measured before (R_0) and after polarization (R_f) by alternating current impedance in the frequency range of 500 kHz to 10 mHz. T_{Li+} was calculated using the following Equation (4):

$$T_{Li+} = \frac{I_{SS}(\Delta V - I_0 R_0)}{I_0\left(\Delta V - I_{SS} R_f\right)} \quad (4)$$

where the current value before direct current polarization (I_0) was calculated using R_{el} from an impedance measurement according to Equation (5). R_{el} is the resistance of Nafion-Li^+-DOL-DME membrane, that was determined from the intercept at active impedance axis of the highest frequency regime of the Nyquist plot. This omits the experimental determination of the initial current I_0 which is obtainable with rather limited accuracy only [42]:

$$I_0 = \frac{\Delta V}{(R_{el} + R_0)} \quad (5)$$

The active paste was prepared by mixing the S/C composite with carbon black (Ketjen Black) and polyvinylidene fluoride (Kynar) dissolved in N-methyl-2-pyrrolidone (mass

ratio of 85/10/5). The slurry was coated on a stainless-steel substrate and then dried in a vacuum oven at 50 °C. The electrodes were pressed under a 1000 kg cm^{-2} pressure and then vacuum-dried at 50 °C for 16 h. The Li–S electrochemical cells were assembled in a high-purity argon-filled glove box with the content of water and oxygen $\leq$ 1 ppm (Spectroscopic Systems, Moscow, Russia). Electrochemical testing with liquid electrolyte and polypropylene film (PP) was carried out in the sealed three electrode cells with a lithium as counter and reference electrodes. 1 M bis(trifluoromethane)sulfonimide lithium ($Li(CF_3SO_2)_2N$, LiTFSI, 3 M Chemicals, Maplewood, MA, USA) in a DOL-DME (1:1 by volume) was used as the electrolyte. The water content in the electrolyte measured by Fischer titration (917 Coulometer, Metrohm, Herisau, Switzerland) did not exceed 30 ppm. The tests of S/C composite in the cells with membrane instead of PP separator were carried out in the sealed two electrode cells with lithium counter electrode. The cyclic voltammetry (CV) results were registered with a P-20X potentiostat (Elins, Chernogolovka, Russia). The chronopotentiometric measurements were carried out with multichannel computer-aided cycler AZVRIK-50-10V (Buster JSC, Moscow, Russia). The values of capacity were calculated on the sulfur content.

3. Results

3.1. S/C Cathode

The specific surface area of the mesoporous carbon used for composite sulfur cathode formation is equal to 1800 m^2 g^{-1}. In the Raman spectra of mesoporous carbon (Figure 1) an intensive band with a maximum at ~1600 cm^{-1} can be appointed to the crystalline graphite (sp^2-hybridized carbon, G-band) and a band at ~1350 cm^{-1} to the disordered graphite (D-band). Together with them, two bands can be identified at ~1200 and ~1530 cm^{-1}, corresponding to the sp^3-hybridized carbon [43]. The contribution of the bands of sp^3-hybridized carbon amounts approximately 40%. This indicates that the mesoporous carbon is represented mainly by a sp^2-hybridized carbon. The specific surface area of S/C composite is equal to 7 m^2 g^{-1}. The sharp decrease in the surface area after sulfur loading indicates that sulfur occupies almost all the pores of mesoporous carbon.

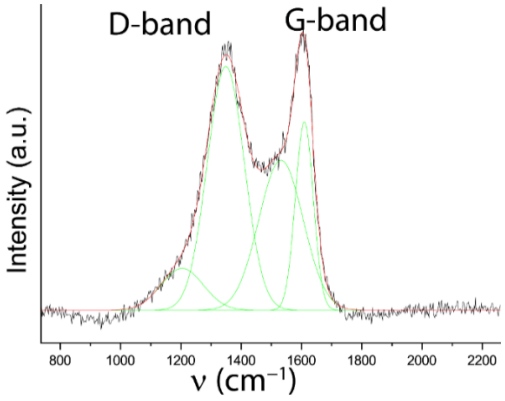

Figure 1. Raman spectra of mesoporous carbon.

The XRD pattern of mesoporous carbon is represented by a broad diffraction peak at 2θ of ~25.7° and a low intensive more broad signal at ~43° (Figure 2). The positions and intensity of the diffraction peaks may be described as carbon (Card 65-6212 PDF-2) as (002), (100) and (101) crystallographic planes. The interplanar spacing calculated from the positions of diffraction maxima at ~25.7° is 0.347 nm that is somewhat higher than interplanar spacing of graphite (0.335 nm) and can be corresponded to the (002) graphene crystallographic plane [44].

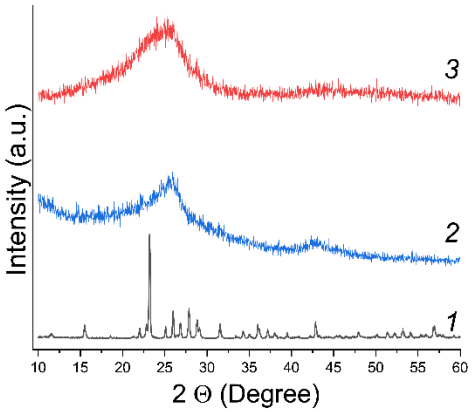

Figure 2. The XRD patterns of the sulfur (1), mesoporous carbon (2) and S/C composite (3). (Adapted from Ref. [45]).

XRD pattern of the S/C composite is a combination of the XRD patterns of sulfur and carbon material of a lower intensity that results in the broad peak in the region of 2θ~22–30° due to the contribution of sulfur and carbon peaks and the decrease in intensity and almost disappearance of the peaks of mesoporous carbon at ~43°. The XRD pattern of the S/C composite contain no intense sharp peaks of S (Figure 2). The disappearance of the peaks of sulfur on XRD pattern could be due to the reduced size of the sulfur after the sulfur loading process and the sulfur encapsulation in the pores of mesoporous carbon that is confirmed by the SEM images (Figure 3). According to CHNS analysis the mass ratio of carbon: hydrogen: sulfur is 29:1 for mesoporous carbon and 105:1:140 for S/C composite. The sulfur content in S/C amount to 56%.

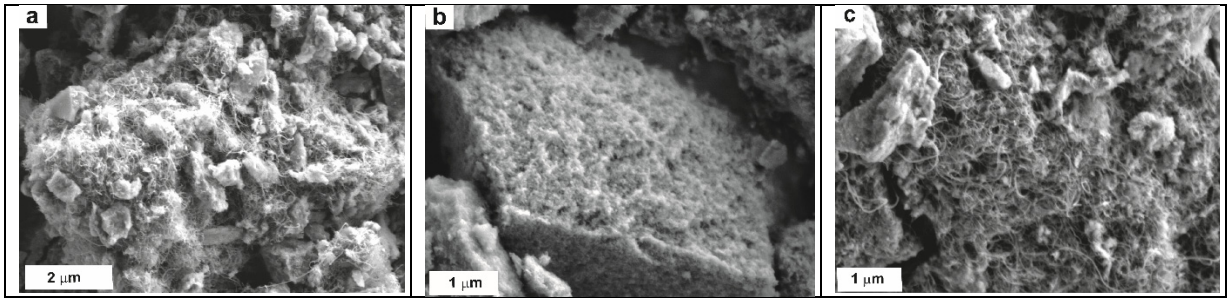

Figure 3. SEM images of the (**a**,**b**) mesoporous carbon and (**c**) S/C composite. (Reprinted from Ref. [45]).

3.2. Membrane

The Nafion membranes obtained after solvation by a DOL–DME mixture for 1 day were a film swollen by 14%, with a thickness of ~190 μm. According to IR spectroscopy (Figure 4), the presence of solvents in the membrane is detected by the characteristic bending vibrations of the C-H bands in the frequency range of 3000–2800 cm^{-1} and by the stretching vibrations of the C-O-C band with a maximum at 865 cm^{-1} [46].

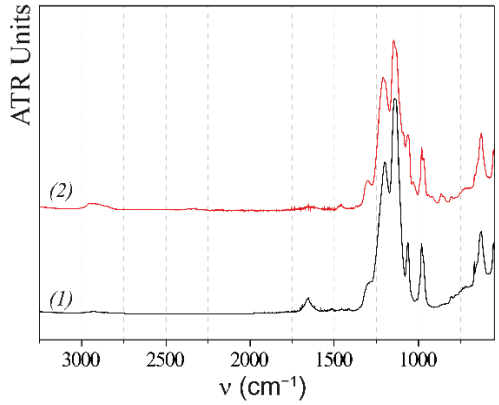

Figure 4. IR spectra of dry (1) and solvated by DOL-DME (2) Nafion-117 membrane.

In the XRD patterns of the dry lithiated Nafion-117 and the membrane solvated by DOL-DME there are two broad signals centered at 2θ~17.5° and~39.9° corresponding to d-spacings of about 0.51 and 0.23 nm (Figure 5). The first broad signal corresponds to the diffraction from the (100) plane of polytetrafluoroethylene (PTFE) (Card № 54-1594) with CF_2-CF_2 chains. The structure of the discussed PTFE chains in Nafion-type polymers is analogical to the PTFE where d-spacings decrease slightly with the equivalent weight increase and approaches the value for PTFE (0.49 nm). The secondary broad peak is associated with the intrachain distances from overlapped peaks from amorphous and crystalline phases [47]. The first broad peak was decomposed into three components. Two of them were attributed to the amorphous phase (2θ~15–16° and 17°) while the curve centered at 2θ~18° was assigned to the crystalline phase [48]. The fraction of the crystalline state X_{cr} in Nafion-117 is found to be approximately 26% which is in agreement with the literature data for Nafion [40]. While X_{cr} is about ~22% for a membrane solvated by DOL-DME. The relative degree of crystallinity of Nafion membranes has been reported to be X_{cr} = 7–30% [47]. It should be noted that X_{cr} calculated from XRD patterns could change from the route of XRD pattern deconvolution (the number of peaks into which decomposition is carried out, the function used, whether the background is subtracted and how). The reported values are in fact a relative degree of crystallinity for qualitative comparison only.

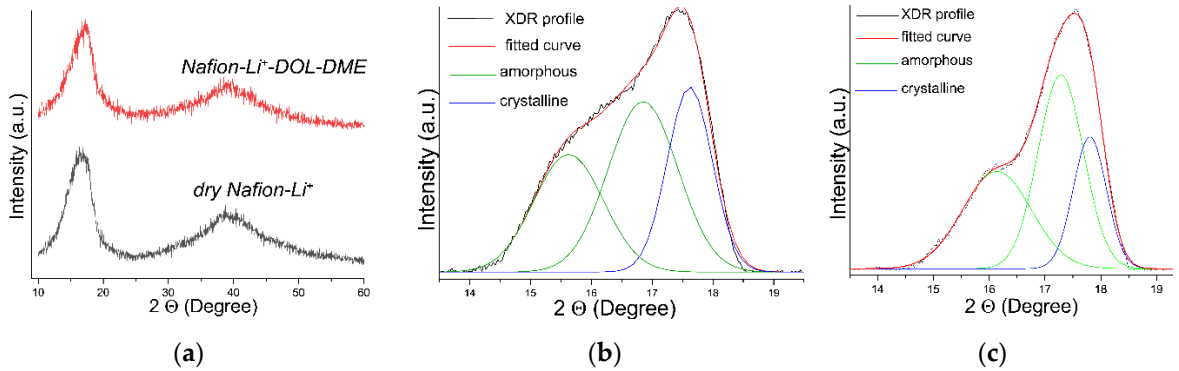

(**a**) (**b**) (**c**)

Figure 5. (**a**) The XRD patterns of dry Nafion-Li^+ and Nafion-Li^+ solvated by DOL-DME Nafion-117 membrane. Nafion-117 membrane. Deconvolution of amorphous and crystalline scattering from (**b**) dry Nafion-Li^+ and (**c**) Nafion-Li^+ -DOL-DME.

The solvation degree of the obtained membranes practically did not change regardless of the number of days the membrane was in contact with DOL-DME and amounted to 1.9 solvent molecules per membrane sulfo-group (Table 1). It should be noted that despite comparable solvent uptake, the ionic conductivity of the membranes solvated for 1 and 5 days differs by 6 times (Table 1). With further Nafion-Li^+ membrane treatment in the

DOL–DME mixture, the conductivity changes within the error of determination. which limit the rate of ion transport in membranes. The data obtained is unusual. In the case of this Nafion-type membranes, the volume of channels that connect the pores is the factor that limits the rate of ionic transport within the membrane. According to previously published data, an increase in membrane conductivity correlates with an increase in the degree of solvation [28]. Another reason for the increase in membrane conductivity may be an increase in the concentration of charge carriers due to the introduction of dopants with a functionalized surface [49]. However, in this case the conductivity increase is observed at the constant solvent uptake and the charge carrier concentration that can be explained by the increase in the mobility of polymer chains when kept in an organic solvent. This observation that the conductivity may increase within some time after complete solvation from the point of view of the conductivity characterization and practical application of solvated cation exchange membranes.

Table 1. The values of ionic conductivity (25 °C), data used for calculating solvation degree and the solvation degree of the Nafion-Li^+-DOL-DME depending on the days during which the membrane was in contact with DOL-DME.

	1 Day	3 Days	5 Days	7 Days	14 Days
σ, S cm^{-1} (25 °C)	$(7.8 \pm 0.4) \times 10^{-8}$	$(8.3 \pm 0.4) \times 10^{-8}$	$(4.4 \pm 0.2) \times 10^{-7}$	$(3.9 \pm 0.2) \times 10^{-7}$	$(4.1 \pm 0.2) \times 10^{-7}$
m_0, mg	30.1	51.5	49.5	35.1	66.4
m, mg	34.2	58.9	56.1	40.1	75.8
Solvation degree	1.8	1.9	1.8	1.9	1.9

It should be noted that Nafion-Li^+ membranes intercalated by the DOL-DME mixture are characterized by a low solvent uptake and, accordingly, low conductivity when compared to membranes with other solvents, such as an ethylene carbonate–propylene carbonate mixture (EC–PC). The result obtained is explained by the low values of the dipole moment of DOL and DME (2.1 and 1.7 D for DOL and DME, respectively) [50,51]. The degree of solvation of the membrane by more polar molecules during the intercalation of the EC-PC mixture was 3.2 (the dipole moments of EC and PC were 4.5 and 5.0 D, respectively) [29]. In addition, EC and PC are characterized by a higher dielectric constant (7.3 and 7.2 for DOL and DME [52,53], 90 and 65 for EC and PC [54], respectively).

High membrane elasticity and strength can be crucial to bear folding during industrial batteries assembly and maintaining battery performance when subjected to deformation [55]. The obtained solvated membrane shows high values of Young's modulus (38 ± 4 MPa), tensile stress (9 ± 1 MPa), and elongation on break (234 ± 15%) (Figure 6), indicating robust network of polymer matrix.

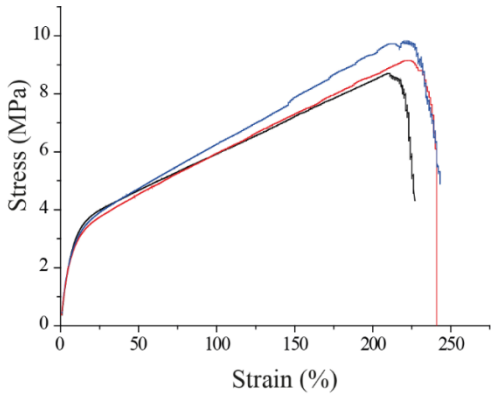

Figure 6. Stress–strain curves of Nafion-117, solvated by DOL-DME.

The conductivity values for Nafion-Li^+-DO-DME are much lower than the conductivity values for the Nafion-212 membrane solvated in 1.0 M $LiCF_3SO_3$ and 0.1 M $LiNO_3$ in the DOL-DME (1:1, volume ratio) solvent [19]. The authors give the value ~ 1.0×10^{-5} S cm^{-1} for the Nafion-212, which was kept in electrolyte for 7 days. We assumed that the lower conductivity values obtained by us may be associated with insufficient solvation of the membrane due to the larger thickness of the Nafion-117 membrane used in this work (thickness of the dry membranes is ~180 and ~50 μm for the Nafion-117 and Nafion-212, correspondingly, with relatively close ion exchange capacities). However, a longer than 5-day aging of the Nafion-117 in DOL-DME mixture does not lead to an increase in the solvent uptake and conductivity. We assumed that the reason why the authors were able to obtain higher conductivity values is the higher solvation due to the treatment of the membrane in the proton form in a DOL-DME salt solution. In this case, the solvation of lithium cations occurs, followed by their introduction into the membrane due to ion exchange. Lithium cations thus drag along solvent molecules into membrane pore. We also carried out an experiment on keeping the proton form of the Nafion-117 membrane in a 1M $LiClO_4$ solution in DOL-DME (1:1) for 2 days. The swelling was estimated to be more than 21% and conductivity at room temperature was 1.3×10^{-4} S cm^{-1}. However, the membrane may have partially dissolved during this treatment. The study of swelling of the proton forms of membranes in saline solutions requires further research.

The DSC curve of the Nafion-Li^+-DOL-DME shows one broad endothermic peak above 50 °C accompanied by the mass loss (Figure 7) due to the evaporation of part of the solvent. Furthermore, there is a bend in the low temperature region beginning at −55 °C. We assumed that it corresponds to the glass transition of the Nafion non-ionic matrix.

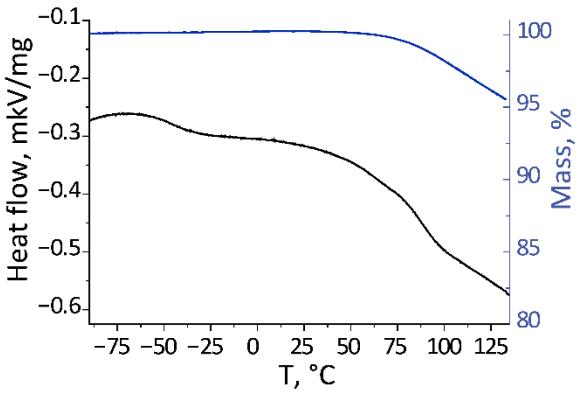

Figure 7. DSC (black line) and TGA (blue line) curve of the Nafion-Li^+-DOL-DME.

The conductivity measurements were performed in the temperature range 0 . . . + 50 °C. At the temperatures below 0 °C, the conductivity is too low which makes it impossible to interpret the impedance spectra. At temperatures above 50 °C, the solvent evaporation is observed according to DSC and TGA data. The impedance spectra of the Nafion-Li^+-DOL-DME at different temperatures is given in Figure 8b. The dependences of the ionic conductivity of the investigated samples on temperature follows the Arrhenius law and are linear in the logσ-1000/T coordinates (Figure 8a) that indicates no phase transitions in the temperature range under consideration. After aging for 14 days, the ionic conductivity is 4.1×10^{-7} S cm^{-1} (room temperature). The value of the activation energy of conductivity is 34 ± 1 kJ mol^{-1}.

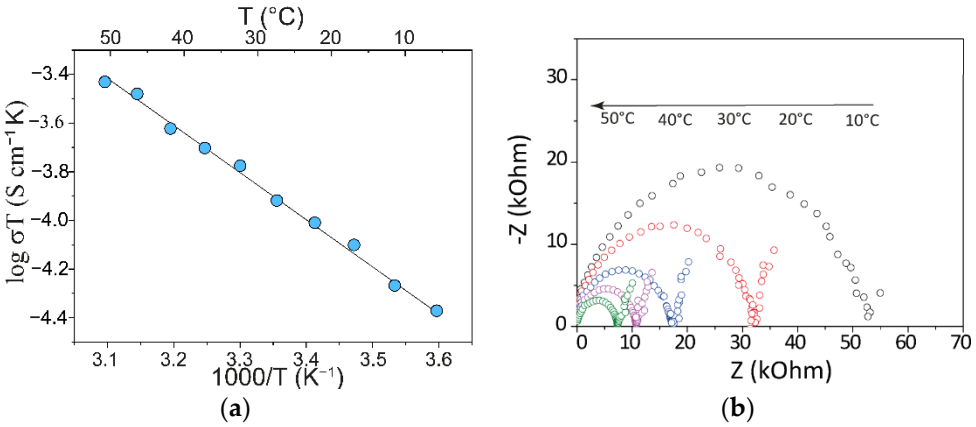

Figure 8. Temperature dependence of ionic conductivity (**a**) and the impedance spectra of the SS/Nafion-Li^+-DOL-DME/SS cell (**b**).

The Li^+ transference number (T_{Li+}) was evaluated by the Bruce-Vincent method (Section 3). The data from Figure 9 listed in Table 2 were inputted into Equations (4) and (5). The calculated value of T_{Li+} was found to be 0.95. That indicates that Li^+ only are carried through the membrane while the SO_3^- fixed on the polymer matrix are immobile. R_{el} was also used for the calculation of membrane conductivity that amounts to 4.3×10^{-7} S cm^{-1}. This value is in good agreement with data obtained from AC impedance spectroscopy for the cell: stainless steel/membrane/stainless steel.

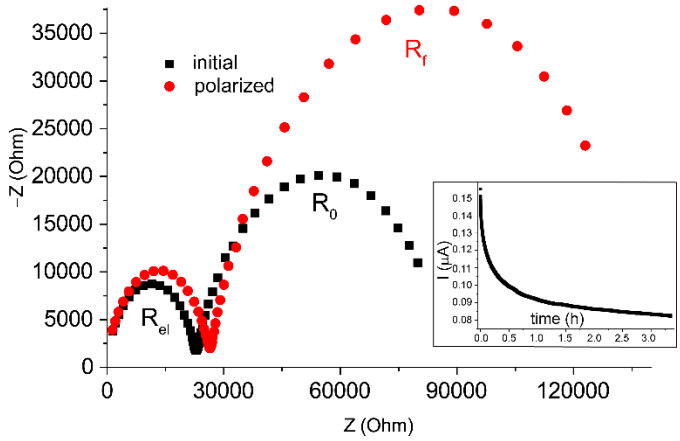

Figure 9. The impedance spectra before and after polarization with DC of the Li/Nafion-Li^+-DOL-DME/Li cell. Inset is chronoamperometry curve at a potential of 10 mV.

Table 2. Data used for the Li^+ transference number calculation.

R_{el}, Ohm.	R_0, Ohm	R_f, Ohm	$I_0 \times 10^{-8}$, A	$I_{ss} \times 10^{-8}$, A
23,133	62,093	108,404	11.73	7.53

3.3. Li–S Battery Testing

CV measurements for Li–S battery cells with PP separator were carried out within a 1.4–3 V potential range. One broad oxidation wave at ~2.4 V and two cathodic peaks at ~2.3 and ~2.0 V (Figure 10a) result from the electrochemical conversion of elemental sulfur and lithium polysulfides (Figure 10a) that is typical for Li–S batteries [2]. The first cycle discharge capacities of S/C composite amount to 730 mAh g^{-1}. During cycling the discharge capacity values decreased rapidly. The discharge capacity was 164 mAh g^{-1} on the 10th cycle (0.1 mV s^{-1}). The decrease of capacities resulting most likely from the dissolution of polysulfides and their transfer to the opposite electrode.

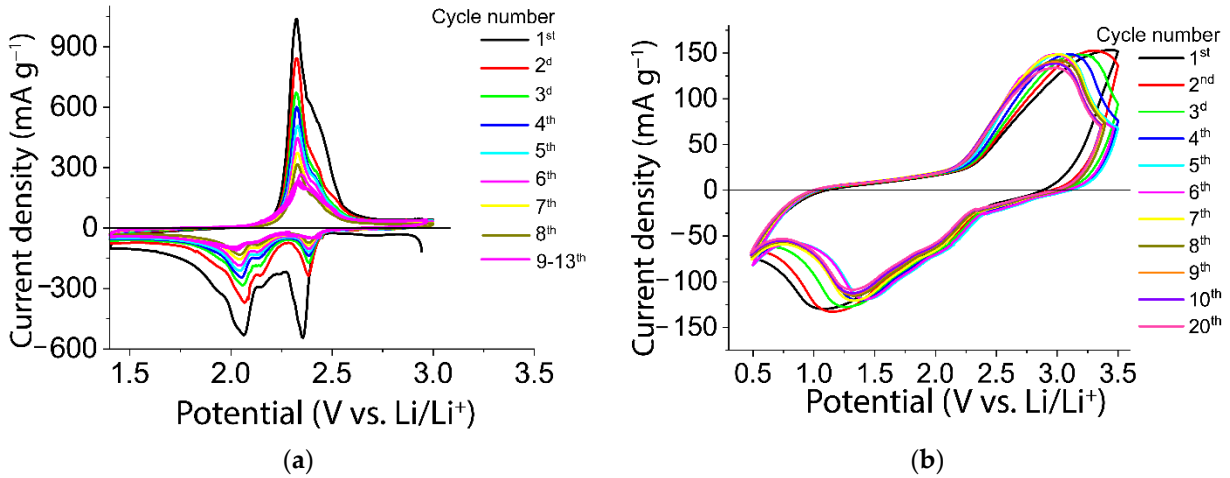

Figure 10. CVs of S/C composite in 1 M LiTFSI in DOL-DME (1:1) in the cell with PP separator (**a**) and with Nafion-Li^+-DOL-DME (**b**). Scan rate is 0.1 mV s^{-1}.

CV measurements for Li–S cells with Nafion-Li^+-DOL-DME instead of PP separator were performed within a 0.5–3.5 V potential range (Figure 10b). The CV curves of the cell with a membrane are different compared with the cell with a PP separator. There are one broad anodic wave at ~3 V and two broad cathodic waves at ~2.1 and ~1.4 V. The peak currents are lower due to the worse kinetics of the battery. The main reason is too high membrane resistance due to its relatively low conductivity and large thickness.

The change in the position of the cathode and anode peaks during cycling (Figure 10b) corresponds to a decrease in the difference between the anode and cathode potentials. This difference reflects the reversibility of the sulfur reduction reaction and the lithium sulfide oxidation reaction, and also depends on the membrane resistance and the resistance at the electrode/Nafion-Li^+-DO-DME interface. We believe that at the beginning of cycling, the resistance at the electrode/Nafion-Li^+-DO-DME interface is higher than during further cycling. Discharge capacity, calculated from CV for the cell with Nafion-Li^+-DOL-DME at the first cycle is 450 mAh g^{-1}. With 10 cycles, no significant changes in peak intensity and potential were observed, that indicates more electrochemical stability of the Li–S cell with the use of membrane. The discharge capacity of S/C in the cell with Nafion-Li^+-DOL-DME reduced to 365 mAh g^{-1} after 10 cycles and to 290 mAh g^{-1} after 40 cycles.

The obtained capacities values are much lower compared to the theoretical capacity of sulfur. This may be due to the high values of the membrane resistance, both due to low conductivity and large thickness of Nafion-117. However, it should be noted that there was a much more stable operation of cells with a membrane compared to a cell with a similar cathode with a PP separator. Thus, the capacity drop of the cell with the PP separator is 78% by the 10th cycle (Figure 11). While a cell with a membrane retains relatively stable capacities when cycling for 40 cycles. The drop in the capacity of the cell with the Nafion-Li^+-DOL-DME membrane is ~19% per 10 cycles. Coulombic efficiency calculated according to the equation (discharge capacity/charge capacity) × 100 is about 86% (average per first 10 cycles). At following 30 cycles, the Coulombic efficiency is closed to 100%.

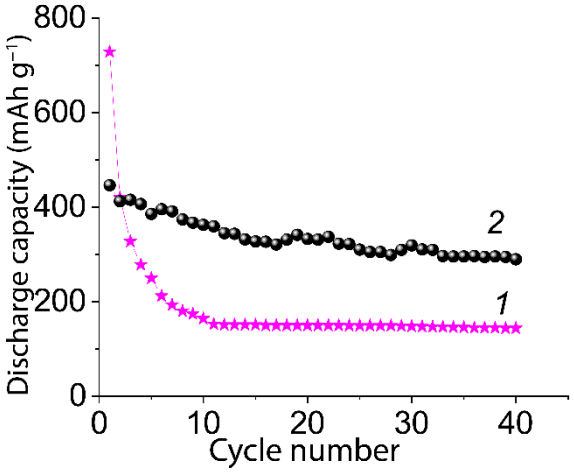

Figure 11. Discharge capacity fading of S/C composite in the cell with PP separator (1) and membrane (2).

Figure 12 shows the results of galvanostatic cycling of the S/C composite in a cell with a PP separator and the cell with the membrane at different current densities. The discharge capacity of the S/C composite in a cell with a PP separator for the first cycle was 1330, 730, and 600 mAh g^{-1} at the current densities of 100, 200, and 400 mA g^{-1}, respectively. However, upon further cycling, the discharge capacity sharply dropped for all current densities, and by the 15th cycle it did not exceed 230 mAh g^{-1} even at the current density of 100 mA g^{-1}. The discharge capacity of the S/C composite in the cell with the membrane in the first cycle was 500, 446, and 190 mAh g^{-1} at the current densities of 100, 200, and 400 mA g^{-1}, respectively, which turned out to be lower than the discharge capacity of the S/C composite in the cell with a PP separator. The degradation of the battery with a membrane electrolyte was much lower as compared to the PP separator. For example, capacity retention was 17% and 85% after 15 cycles at 100 mA g^{-1} for Li–S battery with PP separator and Nafion-Li^+-DOL-DME electrolyte, respectively.

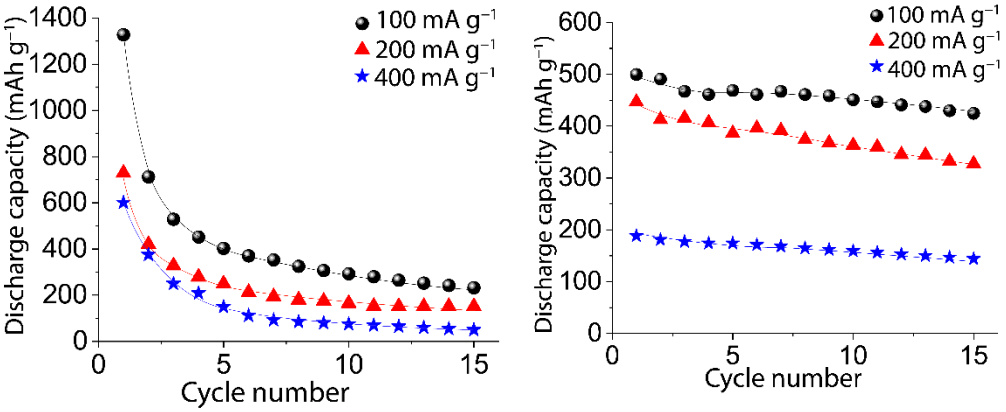

Figure 12. Discharge capacity vs. cycle number of S/C composite in the cell with PP separator (**a**) and membrane (**b**) upon cycling at various current densities.

4. Conclusions

A perfluorosulfonic acid membrane based on Nafion-117 in lithium form intercalated by DOL-DME mixture has been obtained. It was shown that the solvation degree of the obtained membranes practically did not change regardless of the number of days during which the membrane was in contact with DOL-DME and amount to 1.9 solvent molecules per membrane sulfo-group. At the same time, the conductivity increases within 5 days. This observation may be useful for the conductivity characterization and practical application of solvated cation exchange membranes. The ionic conductivity values amount

to ~4 × 10^{-7} S cm^{-1} after 5 days of swelling. Nafion-Li^+-DOL-DME membrane is thermally stable up to 50 °C. The obtained solvated membranes show high values of Young's modulus (38 ± 4 MPa), tensile stress (9 ± 1 MPa), and elongation on break (234 ± 15%). The Li^+ transference number of Nafion-Li^+-DOL-DME membrane is 0.95 indicating that membrane is a single-ion conductor. A comparative study of the electrochemical properties of Li–S batteries with liquid electrolyte (1M LiTFSI in DOL-DME) with a polypropylene film (PP) or Nafion-Li^+-DOL-DME and S/C composite cathodes have shown that the use of a membrane can significantly improve cyclability of the cell.

Author Contributions: Conceptualization, A.B.Y. and S.A.N.; methodology, S.A.N. and T.L.K.; software, S.A.L.; validation, A.B.Y. and T.L.K.; formal analysis, S.A.N.; investigation, S.A.L., D.Y.V. and S.A.N.; resources, A.B.Y. and T.L.K.; data curation, S.A.N.; writing—original draft preparation, S.A.N. and D.Y.V.; writing—review and editing, S.A.N., T.L.K. and A.B.Y.; visualization, S.A.L. and T.L.K.; supervision, A.B.Y.; project administration, A.B.Y.; funding acquisition, A.B.Y. All authors have read and agreed to the published version of the manuscript.

Funding: This work was supported by the Ministry of Science and Higher Education of the Russian Federation as part of the State Assignment of the Kurnakov Institute of General and Inorganic Chemistry of the Russian Academy of Sciences.

Data Availability Statement: Not applicable.

Acknowledgments: This research was performed using the equipment of the JRC PMR IGIC RAS.

Conflicts of Interest: The authors declare no conflict of interest.

References

1. Voropaeva, D.Y.; Safronova, E.Y.; Novikova, S.A.; Yaroslavtsev, A.B. Recent progress in lithium-ion and lithium metal batteries. *Mendeleev Commun.* **2022**, *32*, 287–297. [CrossRef]
2. Yu, X.W.; Manthiram, A. A progress report on metal-sulfur batteries. *Adv. Funct. Mater.* **2020**, *30*, 2004084. [CrossRef]
3. Kang, W.M.; Deng, N.P.; Ju, J.G.; Li, Q.X.; Wu, D.Y.; Ma, X.M.; Li, L.; Naebe, M.; Cheng, B.W. A review of recent developments in rechargeable lithium-sulfur batteries. *Nanoscale* **2016**, *8*, 16541–16588. [CrossRef] [PubMed]
4. Manthiram, A.; Fu, Y.Z.; Chung, S.H.; Zu, C.X.; Su, Y.S. Rechargeable lithium-sulfur batteries. *Chem. Rev.* **2014**, *114*, 11751–11787. [CrossRef] [PubMed]
5. Suzanowicz, A.M.; Mei, C.W.; Mandal, B.K. Approaches to combat the polysulfide shuttle phenomenon in li–s battery technology. *Batteries* **2022**, *8*, 45. [CrossRef]
6. Apel, P.Y.; Bobreshova, O.V.; Volkov, A.V.; Volkov, V.V.; Nikonenko, V.V.; Stenina, I.A.; Filippov, A.N.; Yampolskii, Y.P.; Yaroslavtsev, A.B. Prospects of membrane science development. *Membr. Membr. Technol.* **2019**, *1*, 45–63. [CrossRef]
7. Hyder, A.G.; Morales, B.A.; Cappelle, M.A.; Percival, S.J.; Small, L.J.; Spoerke, E.D.; Rempe, S.B.; Walker, W.S. Evaluation of electrodialysis desalination performance of novel bioinspired and conventional ion exchange membranes with sodium chloride feed solutions. *Membranes* **2021**, *11*, 217. [CrossRef]
8. Ding, D.; Yaroshchuk, A.; Bruening, M.L. Electrodialysis through nafion membranes coated with polyelectrolyte multilayers yields > 99% pure monovalent ions at high recoveries. *J. Membr. Sci.* **2022**, *647*, 120294. [CrossRef]
9. Song, Y.; Zhao, Z. Recovery of lithium from spent lithium-ion batteries using precipitation and electrodialysis techniques. *Sep. Purif. Technol.* **2018**, *206*, 335–342. [CrossRef]
10. Karimi, M.B.; Mohammadi, F.; Hooshyari, K. Recent approaches to improve nafion performance for fuel cell applications: A review. *Int. J. Hydrogen Energy* **2019**, *44*, 28919–28938. [CrossRef]
11. Golubenko, D.V.; Van der Bruggen, B.; Yaroslavtsev, A.B. Ion exchange membranes based on radiation-induced grafted functionalized polystyrene for high-performance reverse electrodialysis. *J. Power Sources* **2021**, *511*, 230460. [CrossRef]
12. Jiang, B.; Wu, L.; Yu, L.; Qiu, X.; Xi, J. A comparative study of nafion series membranes for vanadium redox flow batteries. *J. Membr. Sci.* **2016**, *510*, 18–26. [CrossRef]
13. Golubenko, D.V.; Pourcelly, G.; Yaroslavtsev, A.B. Permselectivity and ion-conductivity of grafted cation-exchange membranes based on uv-oxidized polymethylpenten and sulfonated polystyrene. *Sep. Purif. Technol.* **2018**, *207*, 329–335. [CrossRef]
14. Chen, Y.; Xu, G.; Liu, X.; Pan, Q.; Zhang, Y.; Zeng, D.; Sun, Y.; Ke, H.; Cheng, H. A gel single ion conducting polymer electrolyte enables durable and safe lithium ion batteries via graft polymerization. *RSC Adv.* **2018**, *8*, 39967–39975. [CrossRef] [PubMed]
15. Kulova, T.; Skundin, A.; Chekannikov, A.; Novikova, S.; Voropaeva, D.; Yaroslavtsev, A. Sodium rechargeable batteries with electrolytes based on nafion membranes intercalated by mixtures of organic solvents. *Batteries-Basel* **2018**, *4*, 61. [CrossRef]
16. Evschik, E.Y.; Novikov, D.V.; Berestenko, V.I.; Levchenko, A.V.; Sanginov, E.A.; Dobrovolsky, Y.A. Binder effect on the stability of the thinfilm anodes for lithiumion batteries based on si@sio2 nanoparticles. *Russ. Chem. Bull.* **2016**, *65*, 1986–1989. [CrossRef]

17. Jiang, S.; Lu, Y.; Lu, Y.; Han, M.; Li, H.; Tao, Z.; Niu, Z.; Chen, J. Nafion/titanium dioxide-coated lithium anode for stable lithium-sulfur batteries. *Chem. Asian J.* **2018**, *13*, 1379–1385. [CrossRef]
18. Gao, J.; Sun, C.; Xu, L.; Chen, J.; Wang, C.; Guo, D.; Chen, H. Lithiated nafion as polymer electrolyte for solid-state lithium sulfur batteries using carbon-sulfur composite cathode. *J. Power Sources* **2018**, *382*, 179–189. [CrossRef]
19. Yu, X.; Joseph, J.; Manthiram, A. Polymer lithium–sulfur batteries with a nafion membrane and an advanced sulfur electrode. *J. Mater. Chem. A* **2015**, *3*, 15683–15691. [CrossRef]
20. Bauer, I.; Thieme, S.; Brückner, J.; Althues, H.; Kaskel, S. Reduced polysulfide shuttle in lithium–sulfur batteries using nafion-based separators. *J. Power Sources* **2014**, *251*, 417–422. [CrossRef]
21. Huang, J.-Q.; Zhang, Q.; Peng, H.-J.; Liu, X.-Y.; Qian, W.-Z.; Wei, F. Ionic shield for polysulfides towards highly-stable lithium–sulfur batteries. *Energy Environ. Sci.* **2014**, *7*, 347–353. [CrossRef]
22. Zhuang, T.Z.; Huang, J.Q.; Peng, H.J.; He, L.Y.; Cheng, X.B.; Chen, C.M.; Zhang, Q. Rational integration of polypropylene/graphene oxide/nafion as ternary-layered separator to retard the shuttle of polysulfides for lithium-sulfur batteries. *Small* **2016**, *12*, 381–389. [CrossRef] [PubMed]
23. Babu, D.B.; Giribabu, K.; Ramesha, K. Permselective speek/nafion composite-coated separator as a potential polysulfide crossover barrier layer for li-s batteries. *ACS Appl. Mater. Interfaces* **2018**, *10*, 19721–19729. [CrossRef] [PubMed]
24. Kim, S.H.; Yeon, J.S.; Kim, R.; Choi, K.M.; Park, H.S. A functional separator coated with sulfonated metal–organic framework/nafion hybrids for li–s batteries. *J. Mater. Chem. A* **2018**, *6*, 24971–24978. [CrossRef]
25. Wang, J.; Zhai, P.; Zhao, T.; Li, M.; Yang, Z.; Zhang, H.; Huang, J. Laminar mxene-nafion-modified separator with highly inhibited shuttle effect for long-life lithium–sulfur batteries. *Electrochim. Acta* **2019**, *320*, 134558. [CrossRef]
26. Cao, Y.; Li, X.; Aksay, I.A.; Lemmon, J.; Nie, Z.; Yang, Z.; Liu, J. Sandwich-type functionalized graphene sheet-sulfur nanocomposite for rechargeable lithium batteries. *Phys. Chem. Chem. Phys.* **2011**, *13*, 7660–7665. [CrossRef]
27. Tang, Q.; Shan, Z.; Wang, L.; Qin, X.; Zhu, K.; Tian, J.; Liu, X. Nafion coated sulfur–carbon electrode for high performance lithium–sulfur batteries. *J. Power Sources* **2014**, *246*, 253–259. [CrossRef]
28. Voropaeva, D.Y.; Novikova, S.A.; Yaroslavtsev, A.B. Polymer electrolytes for metal-ion batteries. *Russ. Chem. Rev.* **2020**, *89*, 1132–1155. [CrossRef]
29. Voropaeva, D.Y.; Novikova, S.A.; Kulova, T.L.; Yaroslavtsev, A.B. Conductivity of nafion-117 membranes intercalated by polar aprotonic solvents. *Ionics* **2017**, *24*, 1685–1692. [CrossRef]
30. Liang, H.-Y.; Qiu, X.-P.; Zhang, S.-C.; Zhu, W.-T.; Chen, L.-Q. Study of lithiated nafion ionomer for lithium batteries. *J. Appl. Electrochem.* **2004**, *34*, 1211–1214. [CrossRef]
31. Voropaeva, D.; Novikova, S.; Xu, T.W.; Yaroslaytsev, A. Polymer electrolytes for libs based on perfluorinated sulfocationic nepem-117 membrane and aprotic solvents. *J. Phys. Chem. B* **2019**, *123*, 10217–10223. [CrossRef] [PubMed]
32. Sanginov, E.A.; Kayumov, R.R.; Shmygleva, L.V.; Lesnichaya, V.A.; Karelin, A.I.; Dobrovolsky, Y.A. Study of the transport of alkali metal ions in a nonaqueous polymer electrolyte based on nafion. *Solid State Ion.* **2017**, *300*, 26–31. [CrossRef]
33. Voropaeva, D.Y.; Novikova, S.A.; Kulova, T.L.; Yaroslavtsev, A.B. Solvation and sodium conductivity of nonaqueous polymer electrolytes based on nafion-117 membranes and polar aprotic solvents. *Solid State Ionics* **2018**, *324*, 28–32. [CrossRef]
34. Istomina, A.S.; Yaroslavtseva, T.V.; Reznitskikh, O.G.; Kayumov, R.R.; Shmygleva, L.V.; Sanginov, E.A.; Dobrovolsky, Y.A.; Bushkova, O.V. Li-nafion membrane plasticised with ethylene carbonate/sulfolane: Influence of mixing temperature on the physicochemical properties. *Polymers* **2021**, *13*, 1150. [CrossRef] [PubMed]
35. Krupina, A.A.; Kayumov, R.R.; Shmygleva, L.V.; Nechaev, G.V.; Lapshin, A.N.; Shmygleva, L.V. Polymer electrolytes based on na-nafion plasticized by binary mixture of ethylene carbonate and sulfolane. *Membranes* **2022**, *12*, 840. [CrossRef]
36. Gao, J.; Lowe, M.A.; Kiya, Y.; Abruña, H.D. Effects of liquid electrolytes on the charge–discharge performance of rechargeable lithium/sulfur batteries: Electrochemical and in-situ x-ray absorption spectroscopic studies. *J. Phys. Chem. C* **2011**, *115*, 25132–25137. [CrossRef]
37. McCreary, C.; An, Y.; Kim, S.U.; Hwa, Y. A perspective on li/s battery design: Modeling and development approaches. *Batteries* **2021**, *7*, 82. [CrossRef]
38. Yim, T.; Park, M.-S.; Yu, J.-S.; Kim, K.J.; Im, K.Y.; Kim, J.-H.; Jeong, G.; Jo, Y.-N.; Woo, S.-G.; Kang, K.-S.; et al. Effect of chemical reactivity of polysulfide toward carbonate-based electrolyte on the electrochemical performance of li–s batteries. *Electrochim. Acta* **2013**, *107*, 454–460. [CrossRef]
39. Skulimowska, A.; Dupont, M.; Zaton, M.; Sunde, S.; Merlo, L.; Jones, D.J.; Rozière, J. Proton exchange membrane water electrolysis with short-side-chain aquivion® membrane and iro2 anode catalyst. *Int. J. Hydrogen Energy* **2014**, *39*, 6307–6316. [CrossRef]
40. Kim, H.; Lee, S.; Kim, S.; Oh, C.; Ryu, J.; Kim, J.; Park, E.; Hong, S.; No, K. Membrane crystallinity and fuel crossover in direct ethanol fuel cells with nafion composite membranes containing phosphotungstic acid. *J. Mater. Sci.* **2017**, *52*, 2400–2412. [CrossRef]
41. Evans, J.; Vincent, C.A.; Bruce, P.G. Electrochemical measurement of transference numbers in polymer electrolytes. *Polymer* **1987**, *28*, 2324–2328. [CrossRef]
42. Hiller, M.M.; Joost, M.; Gores, H.J.; Passerini, S.; Wiemhöfer, H.D. The influence of interface polarization on the determination of lithium transference numbers of salt in polyethylene oxide electrolytes. *Electrochim. Acta* **2013**, *114*, 21–29. [CrossRef]
43. Wilcox, J.D.; Doeff, M.M.; Marcinek, M.; Kostecki, R. Factors influencing the quality of carbon coatings on lifepo4. *J. Electrochem. Soc.* **2007**, *154*, A389–A395. [CrossRef]

44. Nethravathi, C.; Rajamathi, M. Chemically modified graphene sheets produced by the solvothermal reduction of colloidal dispersions of graphite oxide. *Carbon* **2008**, *46*, 1994–1998. [CrossRef]
45. Novikova, S.; Voropaeva, D.; Li, S.; Yaroslavtsev, A. S/C composites with different carbon matrices as cathode materials for metal–sulfur batteries. *Eng. Proc.* **2022**, *19*, 28. [CrossRef]
46. Socrates, G. *Infrared and Raman Characteristic Group Frequencies: Tables and Charts*, 3rd ed.; John Wiley Sons LTD: Baffins Lane, UK, 2001; p. 347.
47. Kusoglu, A.; Weber, A.Z. New insights into perfluorinated sulfonic-acid ionomers. *Chem. Rev.* **2017**, *117*, 987–1104. [CrossRef]
48. Moukheiber, E.; De Moor, G.; Flandin, L.; Bas, C. Investigation of ionomer structure through its dependence on ion exchange capacity (iec). *J. Membr. Sci.* **2012**, *389*, 294–304. [CrossRef]
49. Safronova, E.Y.; Stenina, I.A.; Yaroslavtsev, A.B. The possibility of changing the transport properties of ion-exchange membranes by their treatment. *Pet. Chem.* **2017**, *57*, 299–305. [CrossRef]
50. Walker, R.; Davidson, D. The dielectric constant and dipole moment of 1,3-dioxane. *Can. J. Chem.* **1959**, *37*, 492–495. [CrossRef]
51. Yaws, C.L.; Narasimhan, P.K. *Thermophysical Properties of Chemicals and Hydrocarbons. Chapter 19. Dipole Moment—Organic Compounds*; William Andrew Publishing: Norwich, NY, USA, 2009; p. 672. [CrossRef]
52. Wohlfarth, C. *Dielectric Constant of 1,2-dimethoxyethane. Chapter 126. Landolt-Börnstein IV/17: Static Dielectric Constants of Pure Liquids and Binary Liquid Mixtures*; Springer: Berlin/Heidelberg, Germany, 2008; pp. 263–268. [CrossRef]
53. Roy, M.N.; Ekka, D.; Banik, I.; Majumdar, A. Physics and chemistry of lithium halides in 1,3-dioxolane and its binary mixtures with acetonitrile probed by conductometric, volumetric, viscometric, refractometric and acoustic study. *Thermochim. Acta* **2012**, *547*, 89–98. [CrossRef]
54. Liu, Y.; Cai, Z.; Tan, L.; Li, L. Ion exchange membranes as electrolyte for high performance li-ion batteries. *Energy Environ. Sci.* **2012**, *5*, 9007. [CrossRef]
55. Huang, S.; Guan, R.; Wang, S.; Xiao, M.; Han, D.; Sun, L.; Meng, Y. Polymers for high performance li-s batteries: Material selection and structure design. *Prog. Polym. Sci.* **2019**, *89*, 19–60. [CrossRef]